




Article

# The Use of Geographic Databases for Analyzing Changes in Land Cover—A Case Study of the Region of Warmia and Mazury in Poland

Iwona Cieślak <sup>1,\*</sup> , Andrzej Biłozor <sup>1</sup> , Anna Żróbek-Sokolnik <sup>2</sup>  and Marek Zagroba <sup>1</sup>

<sup>1</sup> Department of Socio-Economic Geography, Institute of Spatial Management and Geography, Faculty of Geoengineering, University of Warmia and Mazury in Olsztyn, 10720 Olsztyn, Poland; abilozor@uwm.edu.pl (A.B.); mazag@uwm.edu.pl (M.Z.)

<sup>2</sup> Department of Botany and Nature Protection, University of Warmia and Mazury in Olsztyn, Plac Łódzki, 10727 Olsztyn, Poland; a.zrobsokolnik@uwm.edu.pl

\* Correspondence: isidor@uwm.edu.pl; Tel.: +48-89-523-42-70

Received: 27 March 2020; Accepted: 25 May 2020; Published: 29 May 2020



**Abstract:** This article analyzes the applicability of spatial data for evaluating and monitoring changes in land use and their impact on the local landscape. The Coordination of Information on the Environment (CORINE) Land Cover database was used to develop a procedure and an indicator for analyzing changes in land cover, and the continuity of different land use types. Changes in land use types were evaluated based on land cover data. The results were analyzed over time to track changes in the evaluated region. The studied area was the Region of Warmia and Mazury in Poland. The preservation of homogeneous land cover plays a particularly important role in areas characterized by high natural value and an abundance of forests and water bodies. The study revealed considerable changes in land cover and landscape fragmentation in the analyzed region.

**Keywords:** land cover and land use; geographic databases; CORINE Land Cover; land management; GIS tools

## 1. Introduction

### 1.1. Land Cover and Landscape Fragmentation

Land cover (LC) is the main attribute of space that constitutes a basis for describing the environmental, economic, and social value of a given area [1]. Land cover is generally associated with natural processes that have shaped the local landscape, but in modern times, changes in land cover are increasingly driven by anthropogenic processes. Due to the powerful influence of human activities, land cover is often associated with land use (LU). However, the two concepts are not synonymous [2]. Land use relates to social, economic, and cultural aspects, whereas land cover denotes the physical attributes associated with flora, fauna, and surface elements of natural and anthropogenic origin [3]. In simple terms, two areas with identical land cover can be used in a different manner. For example, an area with forest cover can be used for the production of timber and forestry materials, or for recreational purposes [4]. Land use is not always an accurate and an unambiguous term. Various forms of land use can be encountered in areas with identical land cover, which implies that a given territory can be simultaneously used for different purposes [5].

Despite the above, land cover and land use are closely correlated. In the primary sense, land cover represents the extent to which a given area can serve different functions [6]. However, in modern times, the secondary significance of the correlation between land cover and land use appears to play a more important role, in particular in highly populated regions of the world [7]. In those areas, land cover

is the direct effect of extreme anthropogenic pressure [8,9]. Landscape, or the physiognomy of land surface, is modified by human activities [10,11]. The difference between land cover and land use are less visible in highly populated areas where land use types and human activities can be inferred from land cover.

Various factors drive changes in land cover. Land cover is strongly correlated with social [12], economic [13] and environmental [14] processes as well as technological advances [15]. Changes in agricultural production as well as urbanization, globalization and privatization processes testify to the directions and rate of changes in land cover [16]. Variations in land cover are studied to evaluate the extent of urbanization [17] and changes in agriculture [18]. Land cover is also frequently analyzed in landscape studies [19]. Such analyses are carried out to determine the extent of landscape fragmentation [20].

The conversion of large habitat patches into smaller and isolated segments leads to landscape fragmentation [21]. This process is most visible in urbanized areas and other built-up and intensively used areas, which are fragmented by linear infrastructure such as roads and railway lines ([22–24]). Urbanization and the development of transport networks proceed rapidly, which increases the number of linear infrastructure intrusions into natural ecosystems and contributes to landscape fragmentation [25].

Various indicators have been proposed in the literature to evaluate the threats to biological diversity [26]. These indicators have been described in detail by McGargial and Marks [27] based on the theory of habitat patches and wildlife corridors, and they were interpreted in a strict environmental context. Landscape fragmentation was also analyzed in studies on urban development, privatization of municipal land, and urban densification [28,29].

Landscape fragmentation has substantial effects on the environment; therefore, it is monitored regularly in the European Union [30]. According to a 2019 report of the European Environment Agency (EEA) on landscape fragmentation pressure and trends in Europe, there were around 1.5 fragmented landscape elements per km<sup>2</sup> in the European Union in 2015, marking a 3.7% increase from 2009. Approximately 1.13 million km<sup>2</sup>, which accounts for around 28% of the area of the European Union (EU), was strongly fragmented in 2015, marking an increase of 0.7% from 2009. Agricultural land was most affected by strong fragmentation. The largest proportions of strongly fragmented landscapes were noted in Luxembourg (91%), Belgium (83%), and Malta (70%). Finland and Sweden were least affected by landscape fragmentation in the EU. In 2009–2015, the greatest increase in the area of fragmented landscapes was observed in Croatia, Greece, Hungary, and Poland [31].

The presented data indicate that landscape fragmentation poses a considerable problem in Europe, which is why effective methods for monitoring the relevant phenomena are needed. Such methods have already been implemented at the national and supranational level, but very few studies have investigated landscape fragmentation at the regional and local level. It should be noted that most planning decisions that directly contribute to landscape fragmentation are made by regional and local authorities.

Many indicators for evaluating the extent of landscape fragmentation rely on land cover [32]. These tools can be deployed in studies analyzing urbanization processes and the structure of agricultural land to evaluate changes in ecosystems and the urban fabric. In the presented study, the landscape fragmentation theory was used to evaluate changes in land cover in a holistic approach. In this novel approach, the proposed indices can be applied to evaluate fragmentation across all types of land cover. Indicators of land fragmentation can provide valuable information about landscape changes and the severity of anthropogenic pressure [33,34]. Land fragmentation can be evaluated with the use of indicators of land use continuity, which are applied to investigate landscape continuity in urban areas [35,36].

The main novelty of the presented research is the methodical approach to landscape fragmentation. This process was analyzed not only from an environmental perspective, but also in view of all land cover types identified in the CLC database to evaluate changes in land use in the studied region.

Changes in agricultural operations, uncontrolled urbanization, and fragmentation of property rights were included in the analysis.

### 1.2. Sources of Data on Land Cover

Technological advancement and progression of knowledge have contributed to the popularity and ease of research into land cover [37]. Considerable progress has also been made in geographic research. Environmental, cultural and economic data linked to geographic locations support detailed analyses and the formulation of conclusions regarding spatial processes [38]. Land surface images acquired with unprecedented frequency and resolution are a rich source of information [39]. Satellite images processed with photogrammetric techniques also expand our knowledge about land cover and support the formulation of conclusions regarding spatial processes [40]. The development of Geographic Information System (GIS) applications created access to vast sources of land data [41,42]. These resources are highly useful for monitoring changes in space [43]. However, the quality of land data can differ considerably.

Remote sensing instruments support high-resolution analyses of land cover [44,45] and evaluations of changes in land use in areas that are directly exposed to urbanization pressure [46–50]. They are used to monitor changes in human activities [51,52] and urban ecological land cover (UELC), and they contribute to crisis management by supplying vital data for generating maps, monitoring the environment, managing disasters, and enhancing the capabilities of civilian and military data gathering systems [53]. Changes in land use caused by urbanization are evaluated based on very high-resolution satellite images (VHR) [54–56], synthetic-aperture radar (SAR) images [57], nighttime light (NTL) images [58–61], greenhouse gas emission data [62,63], and vegetation data (such as the normalized difference vegetation index, NDVI) [64]. Anthropogenic and natural changes in land use are also mapped and monitored with the use of Urban Atlas data [65–68]. However, most of these resources are limited due to differences in continuity, accuracy, and cyclicity of data describing various land cover types. These problems are addressed by overlaying land cover maps and using data from various sources [69–73]. A similar approach is used by the EEA, which relies on Copernicus High Resolution Layers (HRL) satellite imagery to classify landscape fragmentation. However, satellite images are not always complete, and some areas are not assigned Imperviousness Degree values (IMD) due to cloud cover [74].

Data that cover large areas, and are accumulated in a consistent manner with the use of the same techniques, are most valuable [75]. Information that is acquired and released periodically facilitates analyses of spatial phenomena as well as their dynamics [76].

The Coordination of Information on the Environment (CORINE) Land Cover database is a thematic component of the CORINE system, which supports the collection and analysis of geospatial information. The CORINE Land Cover (CLC) inventory is a European initiative that was introduced in all countries of the European Community in 1985. This pan-European program was implemented in Poland by a decision of the Chief Inspector of Environmental Protection in 2001. The CLC initiative was established to pursue the following objectives:

- acquire and synchronize interdisciplinary data on the state of the environment with the main focus on priority areas in each Member State of the European Community;
- harmonize and coordinate the organization and management of data at the local and international level;
- guarantee the compatibility of the gathered data.

The CLC database is a tool for conducting complex spatial analyses based on diverse land use types. An analysis of CLC data indicates that the European continent is characterized by considerable spatial continuity; therefore, this inventory can be used to identify various types of land cover [77]. One of the greatest advantages of the CLC dataset is that it is regularly updated, which makes this resource particularly useful for analyzing the rate of changes in land use and to develop forecasts.

CLC data covering for 2006, 2012, and 2018 were analyzed in this study. It should also be noted that the CLC inventory is a more versatile tool than other sources of geospatial information, such as the Urban Atlas of the Global Human Settlement Layer [78].

The CORINE Land Cover (CLC) inventory was initiated in 1985 (reference year 1990) as part of the Copernicus GIO Land Monitoring 2011–2013 program. GIO-land is an operational project of European Copernicus programme that aims at producing several land cover dataset using satellite images. The inventory is updated every six years in nearly all European countries. Previous updates took place in 2000 (CLC2000), 2006 (CLC2006), 2012 (CLC2012), and 2018 (CLC2018). Land cover is inventoried in 44 classes. The Minimum Mapping Unit for aerial phenomena is 25 hectares, and the minimum mapping width for linear phenomena is 100 meters [79]. The CLC is characterized by territorial and methodological continuity, and it is one of the most popular sources of data for research, industry, education, environmental protection and many areas of the economy [80]. The main limitation of CLC resources is the level of detail of source data. CORINE Land Cover is a highly useful resource for small-scale studies, but its applicability for large-scale analysis is debatable. The differences in the area of various land cover types determined with the use of orthophotomaps and CLC data generally do not exceed 10% [81].

The main advantage of the CLC inventory is that it is regularly updated in most European countries. In turn, the Urban Atlas (UA) contains far more detailed data. The UA database classifies high-resolution satellite images (SPOT 2.5 m, ALOS 2.5 m, RapidEye 5 m), which supports the separation of the main coverage classes. Land cover is interpreted with the use of additional data. The smallest mapping unit is 0.25 hectares with an estimated accuracy of 5 m, which supports the generation of land cover maps for only 305 large European cities with a population higher than 100,000. The UA classifies the mapped areas into only 20 land cover classes, which is far less than CLC [82]. However, other inventories are even less informative. Changes in land cover often occur gradually, and they may not be reliably captured in research [83]. These limitations suggest that the CLC inventory is a useful resource for studies conducted on the regional scale.

Land cover data are applied in various types of research, in particular in environmental studies [84]. They are also useful for investigating changes in land fragmentation in areas with various land cover types [85,86]. Simple inventories where data are classified into different land cover classes are effective tools for monitoring local and regional changes in land use, and they provide the local authorities with support in making short-term decisions with long-term consequences.

## 2. Materials and Methods

### 2.1. Study Area

The authors assumed that the analyzed area should be characterized by a high risk of landscape fragmentation without a single identifiable cause. The study area should be characterized by low levels of urbanization and the absence of a large city that could intensify urbanization processes. Therefore, the authors searched for an area with high natural value as well as diverse forms of land use, such as agricultural land used for various purposes, industrial areas, small urban areas, and areas with emerging industrial infrastructure.

The above requirements were met by the Region of Warmia and Mazury in northeastern Poland. The analyzed region has an area of 24,173.47 km<sup>2</sup> and a population of 1.43 million. Farmland is the predominant land cover type with an estimated 52.5% share, including arable land (36.4%) and grassland (more than 16%). Forests and areas with tree cover account for nearly 33%, and surface water bodies for around 5% of the studied region [87,88]. A topographic map of the studied region and its location in Poland are presented in Figure 1.

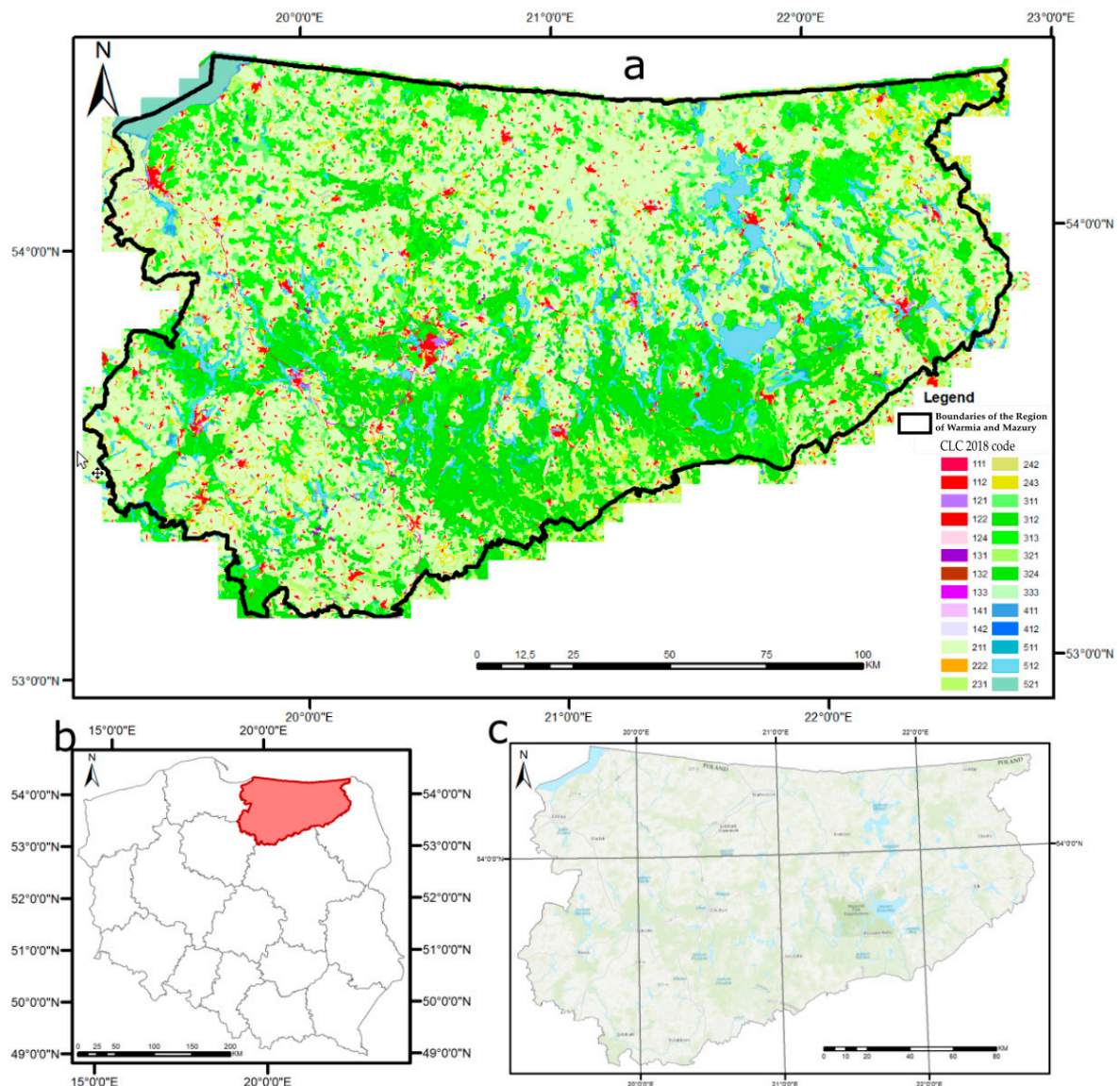


**Figure 1.** Map of the Region of Warmia and Mazury with land cover classes according to CLC2018 (a); the location of the analyzed region on the map of Poland (b); a topographic map of the analyzed region with a cartographic grid in the ETRS\_1989\_Poland\_CS92 system (c).

Strategic documents and research results indicate that the analyzed region is undergoing rapid development, which could contribute to landscape fragmentation [89–91]. According to the EEA report [31], Poland is a country with one of the highest rates of landscape fragmentation. An analysis of landscape fragmentation maps for Europe, which are published as web maps by the EEA based on Copernicus imperviousness layers and TomTom TeleAtlas datasets as fragmenting geometries [26], points to different levels of landscape fragmentation in the Region of Warmia and Mazury. However, these observations were made by evaluating the fragmentation of areas with natural cover. The Effective Mesh Density (seff) is a measure of the degree to which movement between parts of the landscape is interrupted by a Fragmentation Geometry (FG). Fragmentation geometries are defined as the presence of impervious surfaces and traffic infrastructure, including medium-sized roads. The more FGs fragment the landscape, the higher the effective mesh density, hence the higher the fragmentation [74].

The web map in Figure 2 points to high and varied fragmentation, which indicates that the Region of Warmia and Mazury fulfills the research criteria. The studied area was divided into 1061 square equivalent units of measurement (EUM) with a side length of 5 km each. The map of the region with a

division into EUM is presented in Figure 3. The size of EUM supported detailed analyses of changes in the value of the land cover continuity (LCC) indicator in each field. The EUM had to be large enough to ensure the readability of variations in each field. The smallest mapping unit in the CLC inventory is 0.25 hectares. This value was multiplied by 100 to obtain the primary field. The evaluated region was divided into square fields with an area of 2500 ha each, which supported an analysis of variations in each primary field. The process of dividing the evaluated region into primary fields and the number of CLC land cover types in EUM are presented in Figure 3.

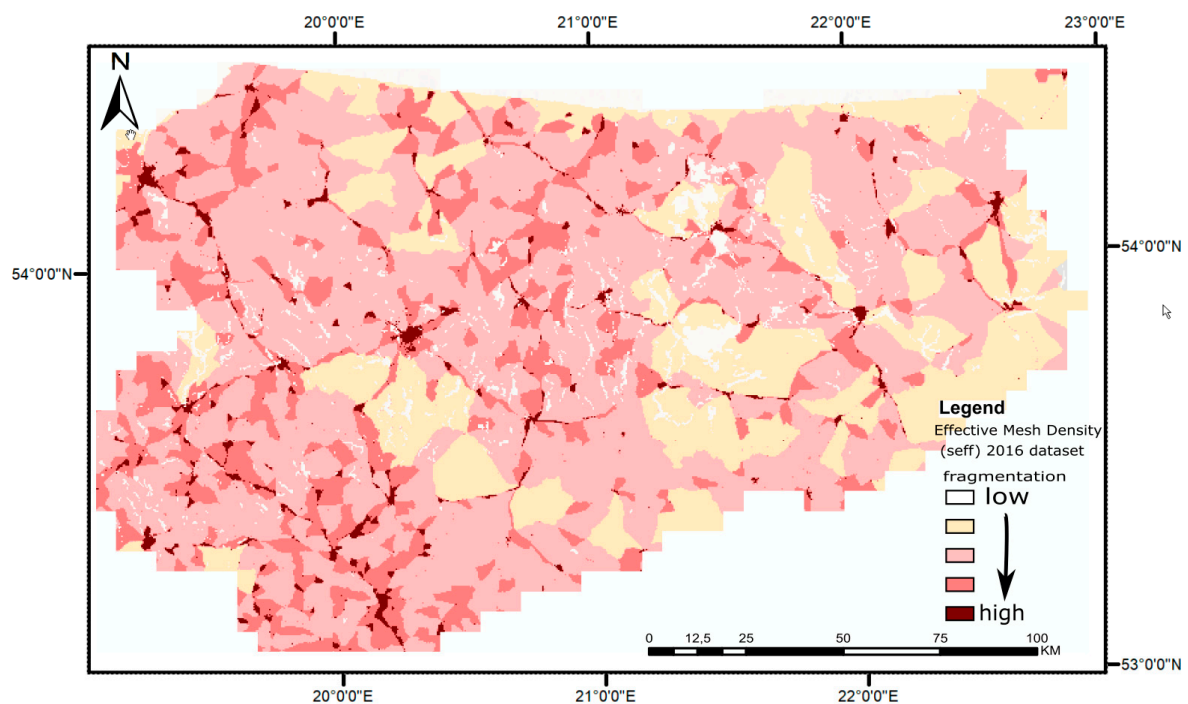


**Figure 2.** Fragmentation status and trends—web map generated by the European Environment Agency (EEA).

## 2.2. Procedure

The analytical procedure was conducted in several stages. Land cover data for 2006, 2012, and 2018 were obtained for the analyzed region. Land cover in the studied area was determined. Evaluations of land cover continuity should rely on spatial units that are uniform in terms of size. Areas with homogeneous land cover should be generated for such units. In the next step, measures of homogeneity should be developed for every unit. An analysis of homogeneity measures and their values over time supports observations of trends in land cover change in the analyzed area. The analytical procedure is presented graphically in Figure 3.

The key research assumptions were formulated in stage 1. The research hypothesis states that land cover databases can provide information about the directions and extent of changes in land cover. The research hypothesis was used to formulate the research objective, which was to determine the applicability of GIS databases for evaluating LC change.

The territorial scope of the study was determined in stage 2. An analysis of various LC databases (CORINE Land Cover, Urban Atlas, and the Global Human Settlement Layer) revealed that the study should cover a large area (at least a region) with different land use types [92–94]. The studied area was the Region of Warmia and Mazury, which is characterized by varied land use and land cover. The region features areas of high natural value (lakes, forests) as well as farmland. Several dynamically growing cities: Olsztyn, Elbląg, and Elk are situated in Warmia and Mazury. Considerable transit traffic passes through the region, mainly via national roads No. 7 and 16.

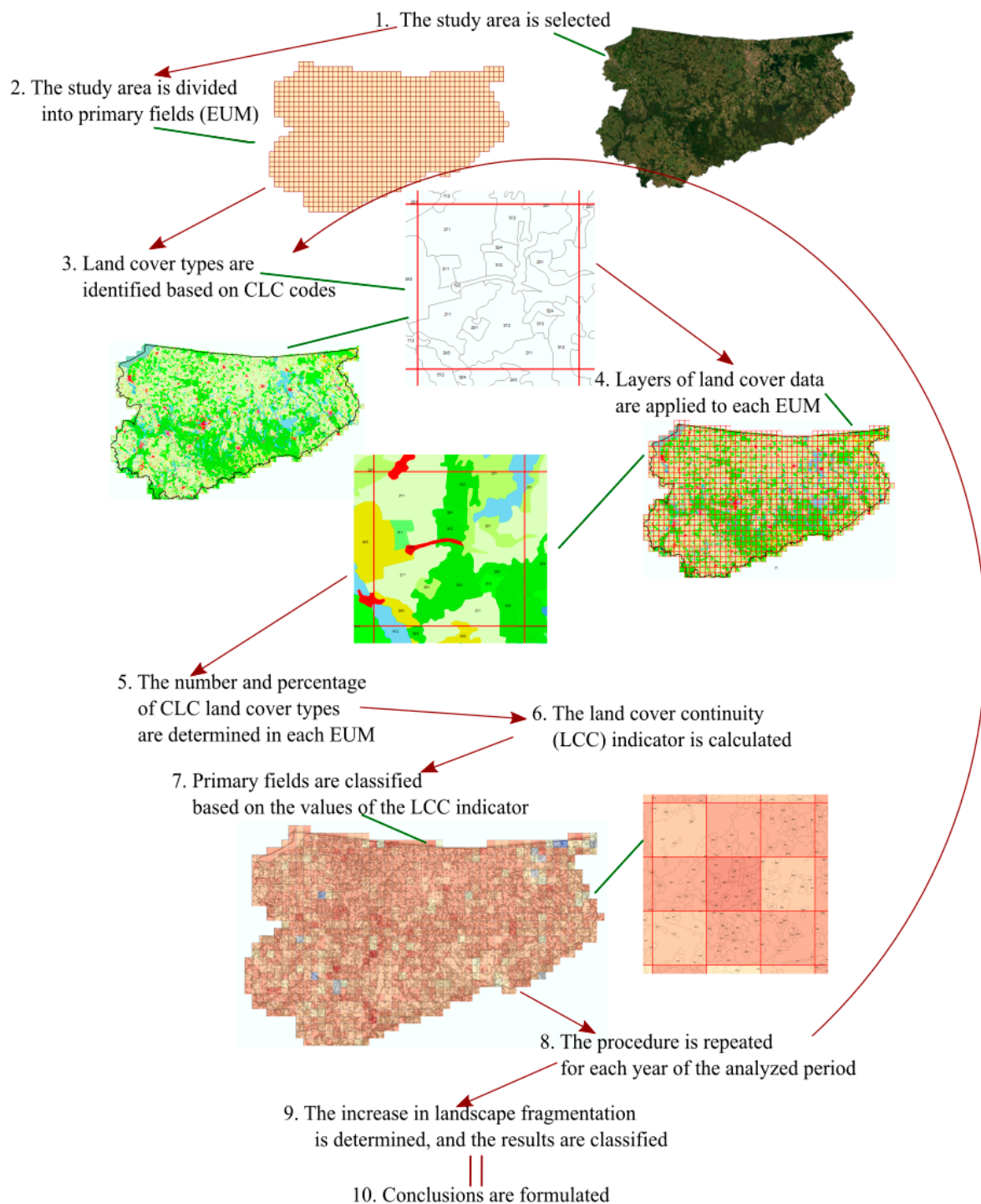


**Figure 3.** Procedure of using the Coordination of Information on the Environment (CORINE) Land Cover (CLC) data to analyze changes in land cover.

The region was divided into EUM to classify different fragments of the studied area. A grid of square primary fields with an area of 25 km<sup>2</sup> each was used, and each field was regarded as an equivalent unit of measurement. The size of EUM supported detailed analyses and the identification of different land cover types.

Data were collected in the next stage of the study. The content and scope of various databases were evaluated, and the CLC database was selected for the present research. The CLC database supported the identification of various types of land cover in the analyzed region as well as changes in

this parameter over time. The collected data for 2006, 2012, and 2018 were processed for each EUM with the use of GIS tools.

An indicator for analyzing the studied phenomenon was developed in stage 5. An indicator of land cover continuity (LCC) was applied due to its broad information content. The method of calculating the LCC indicator is discussed in Section 2.2. The LCC indicator for the analyzed EUM was developed based on data for 2006, 2012, and 2018.

The results were processed and the resulting conclusions were formulated in stage 6. The variations in the LCC indicator across the compared time periods and land cover types were discussed to determine the trends and the extent of changes in land cover.

The continuity of land cover in EUM and the number of identified land cover types play a key role in analyses of changes in land cover [95]. The LCC indicator was applied to describe the continuity of each EUM and to compare the selected EUM. The LCC indicator is a modified version of the indicator of landscape homogeneity proposed by W. Marzęcki [96]. The LCC indicator was developed by modifying the Shannon diversity index (H) which is widely used in landscape fragmentation studies. Modifications were required to adjust the range of indicator values for the needs of this study. Shannon's H is derived from information theory, and it can be applied to measure variations in land cover [97]. The value of Shannon's H ranges from 0 to the natural logarithm ( $\ln$ ) of the number of patches identified in the evaluated area. The indicator was modified by adopting a constant range of values from 0 to 100, and  $\ln$  was replaced by the squared proportion of all land cover types identified in a primary field. This approach was adopted to compare the results across the entire region. The LCC indicator was calculated with the below formula:

$$LCC_n = \sum_{i=1}^m LSC_i^2 \times 100 \quad (1)$$

where:

LCC—indicator of land cover continuity;

$n$ —equivalent unit of measurement (EUM);

LSC—proportion of the  $i^{\text{th}}$  land cover type in the EUM;

$m$ —number of land cover types in the EUM.

The LCC indicator can adopt values in the range of (0,100>). Values close to 0 are indicative of numerous land cover types in EUM, where each LC type accounts for a small fraction of the area, without a clearly dominant LC type. Values close to 100 are indicative of a dominant type of land cover in EUM. Values equal to 100 denote a single type of land cover in EUM. The variations in value of the LCC indicator are presented in Table 1.

The data in Table 1 show that the LCC indicator is determined by the proportions of each land cover type as well as land cover types that clearly dominate over the remaining types.

**Table 1.** Variations in the land cover continuity (LCC) indicator resulting from the number and proportions of different land cover (LC) types in equivalent units of measurement (EUM)—examples.

LSC										Total	LCC
$i$	$i + 1$	$i + 2$	$i + 3$	$i + 4$	$i + 5$	$i + 6$	$i + 7$	$i + 8$	$i + 9$		
0.1	0.1	0.1	0.1	0.1	0.1	0.1	0.1	0.1	0.1	1	10
	0.2	0.1	0.1	0.1	0.1	0.1	0.1	0.1	0.1	1	12
		0.3	0.1	0.1	0.1	0.1	0.1	0.1	0.1	1	16
			0.4	0.1	0.1	0.1	0.1	0.1	0.1	1	22
				0.5	0.1	0.1	0.1	0.1	0.1	1	30
					0.6	0.1	0.1	0.1	0.1	1	40
						0.7	0.1	0.1	0.1	1	52

Table 1. Cont.

LSC										Total	LCC
<i>i</i>	<i>i + 1</i>	<i>i + 2</i>	<i>i + 3</i>	<i>i + 4</i>	<i>i + 5</i>	<i>i + 6</i>	<i>i + 7</i>	<i>i + 8</i>	<i>i + 9</i>		
							0.8	0.1	0.1	1	66
								0.9	0.1	1	82
									1	1	100
					0.2	0.2	0.2	0.2	0.2	1	20
						0.4	0.2	0.2	0.2	1	28
							0.6	0.2	0.2	1	44
								0.8	0.2	1	68
					0.5	0.2	0.1	0.1	0.1	1	32
						0.5	0.3	0.1	0.1	1	36
						0.5	0.2	0.2	0.1	1	34
							0.5	0.3	0.2	1	38
								0.5	0.5	1	50
							0.5	0.4	0.1	1	42
						0.6	0.2	0.1	0.1	1	42
							0.6	0.2	0.2	1	44
							0.6	0.3	0.1	1	46
								0.6	0.4	1	52
						0.7	0.1	0.1	0.1	1	52
							0.7	0.2	0.1	1	54
							0.8	0.1	0.1	1	66
								0.9	0.1	1	82

### 2.3. Data

Data for the analysis were obtained from the CORINE Land Cover database. The CLC is not a new research undertaking in Poland. The project was implemented by the Institute of Geodesy and Cartography between 1990 and 2018 with financial assistance from the EU Structural Funds. The goals of the project have been achieved, and the results are described on the website of the Chief Inspectorate of Environmental Protection ([clc.gios.gov.pl](http://clc.gios.gov.pl)).

The CLC lists every type of land cover in Europe. Unclassified land is not catalogued under any of the headings, which facilitates analyses [98,99]. Land cover and land use are the main categories of information in this inventory [100,101].

In the database, land cover nomenclature is organized at three levels. The first level indicates the five major categories of land cover. The second level features items that make a reference to first-level categories, and the third level contains headings that make a reference to second-level items. As a result, specific land cover types are denoted by three-digit codes, where each digit represents the respective level in the database. The five major land cover categories with the corresponding lower-tier categories are presented below [102]:

1. Urbanized areas—developed areas, including residential, commercial, and industrial areas, mines and green areas in cities.
2. Agricultural areas—all categories of agricultural land, such as arable land, pastures, meadows as well as farmland covered by native vegetation.
3. Forests and semi-natural areas—forests, areas covered by trees and shrubs, as well as open areas with little or no vegetation in forest systems.
4. Wetlands—this category includes land that is highly saturated with water, including marshes, swamps, peat bogs, as well as intertidal flats and salt marshes.
5. Water bodies—marine and inland waters.

The third and most detailed class features 44 land cover types [103]. The study involved CLC data for 2006, 2012, and 2018 to preserve the continuity of aerial images in the process of identifying different land cover types. The CLC database contains satellite images of comparable accuracy and thematic scope [104].

### 3. Results

The LCC indicator for every EUM was calculated based on CLC data for 2006, 2012, and 2018. Based on the calculated values of the LCC indicator, EUM were divided into five identically sized classes. According to the Jenks natural breaks classification method [104], the number of classes should range from 5 to 9. This approach was adopted in this study. The number of classes and their relative ranges guaranteed the highest readability of results and effective identification of spatial processes. The classification system based on the Fisher–Jenks algorithm [105] was assessed with the use of the tabular accuracy index (TAI) [106], and the value of the indicator was highest (0.76) when data were divided into five classes with equal ranges. Class ranges and the number of EUM in each class and year of the analysis are presented in Table 2.

**Table 2.** Classes of the LCC indicator.

	Number of EUM in Each Class					Total
	1	2	3	4	5	
Range of values	>0.81	(0.63; 0.81>	(0.45; 0.63>	<0.25; 0.45>	<0.25	
2006	23	100	202	341	396	1062
2012	21	96	189	318	438	1062
2018	23	87	187	307	458	1062

The classes corresponding to different values of the LCC indicator in the evaluated region are presented in Figure 4. The distribution of classes with the corresponding values of the LCC indicator based on CLC data for 2018 is presented in the largest map. Such evaluations were performed for each year to visualize which LC types were associated with low values of the LCC indicator.

The results were used to calculate the increase in the LCC indicator in 2006–2012 and 2012–2018. The calculated increase was also divided into classes using the same approach. In this case, TAI was highest when data were divided into six classes with equal ranges. Class 6 was composed of EUM with high negative values of increase in the LCC indicator (below  $-0.39$ ). The upper boundary of class 5 was set at 0.00, which was a key value in this classification. The range of values in each class and the number of EUM in each class and year are presented in Table 3. The results of the classification are visualized in Figure 5.

**Table 3.** LCC classes.

	Number of EUM in Each Class						Total
	6	5	4	3	2	1	
Range of values	< $-0.39$	< $-0.39$ ; 0.00>	(0.00; 0.40>	(0.40; 0.80>	(0.80; 1.20>	>1.20	
2006–2012	56	656	308	29	11	2	1062
2012–2018	20	746	273	19	3	1	1062
2006–2018	2	770	290	0	0	0	1062

The results of the study are summarized in Figure 5, which points to a steep increase in the values of the LCC indicator in the central-western part of the analyzed region. The LCC indicator increased at a higher rate in 2012–2018 (Figure 5c) than in 2006–2012 (Figure 5b), which suggests that landscape fragmentation continues to increase, and can be expected to intensify in the future. The data in Figure 5 also indicate that landscape fragmentation is a long-term process and that its real magnitude can be inferred only from long-term observations (Figure 5a).

The statistical parameters of the LCC indicator and the increase in indicator values are presented in Table 4.

**Table 4.** Statistical parameters of the LCC indicator and the increase in indicator values.

	<i>LCC</i>			$\Delta LCC$		
	2006	2012	2018	2006–2012	2012–2018	2006–2018
Min	0.07	0.06	0.06	−0.75	−0.62	−0.42
Max	1.00	1.00	1.00	1.49	1.26	0.39
Mean	0.37	0.35	0.35	−0.02	−0.01	−0.02

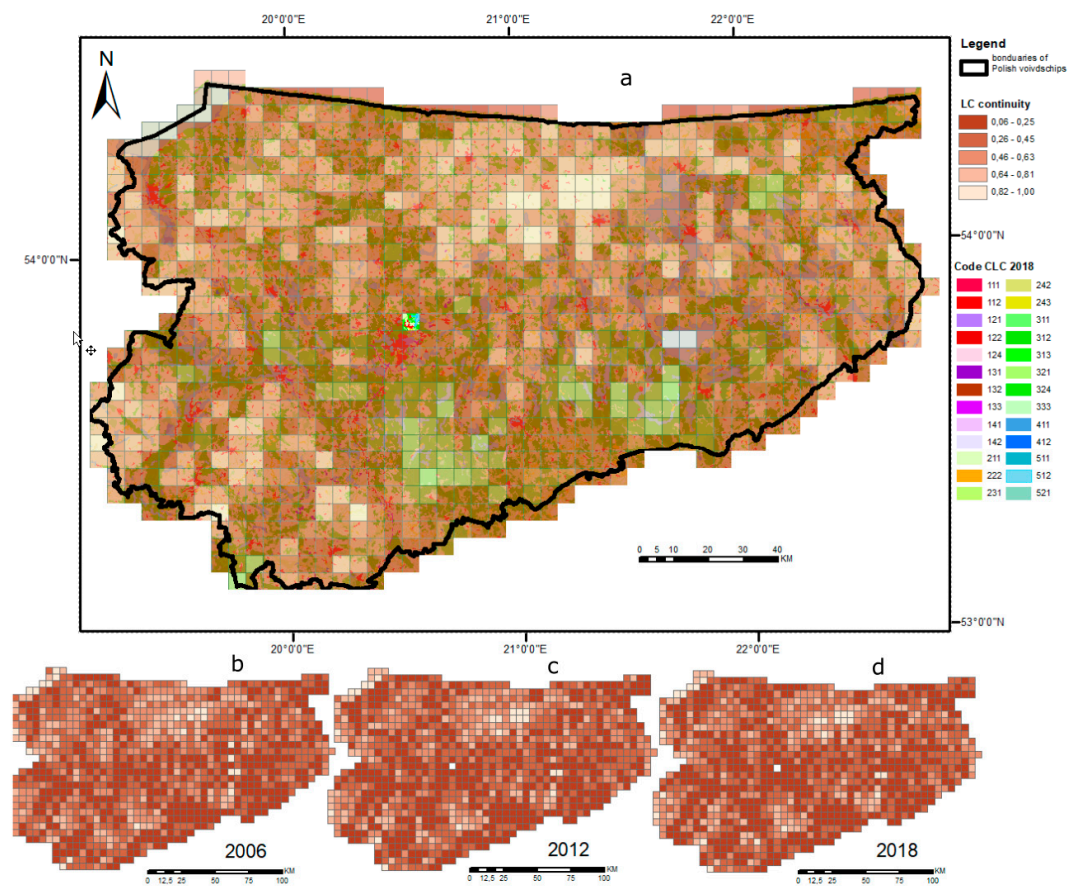


**Figure 4.** Classification of the LCC indicator. (a) classification for 2018 based on CLC data; (b–d) classification of the LCC indicator based on data for 2006 (b), 2012 (c), and 2018 (d).

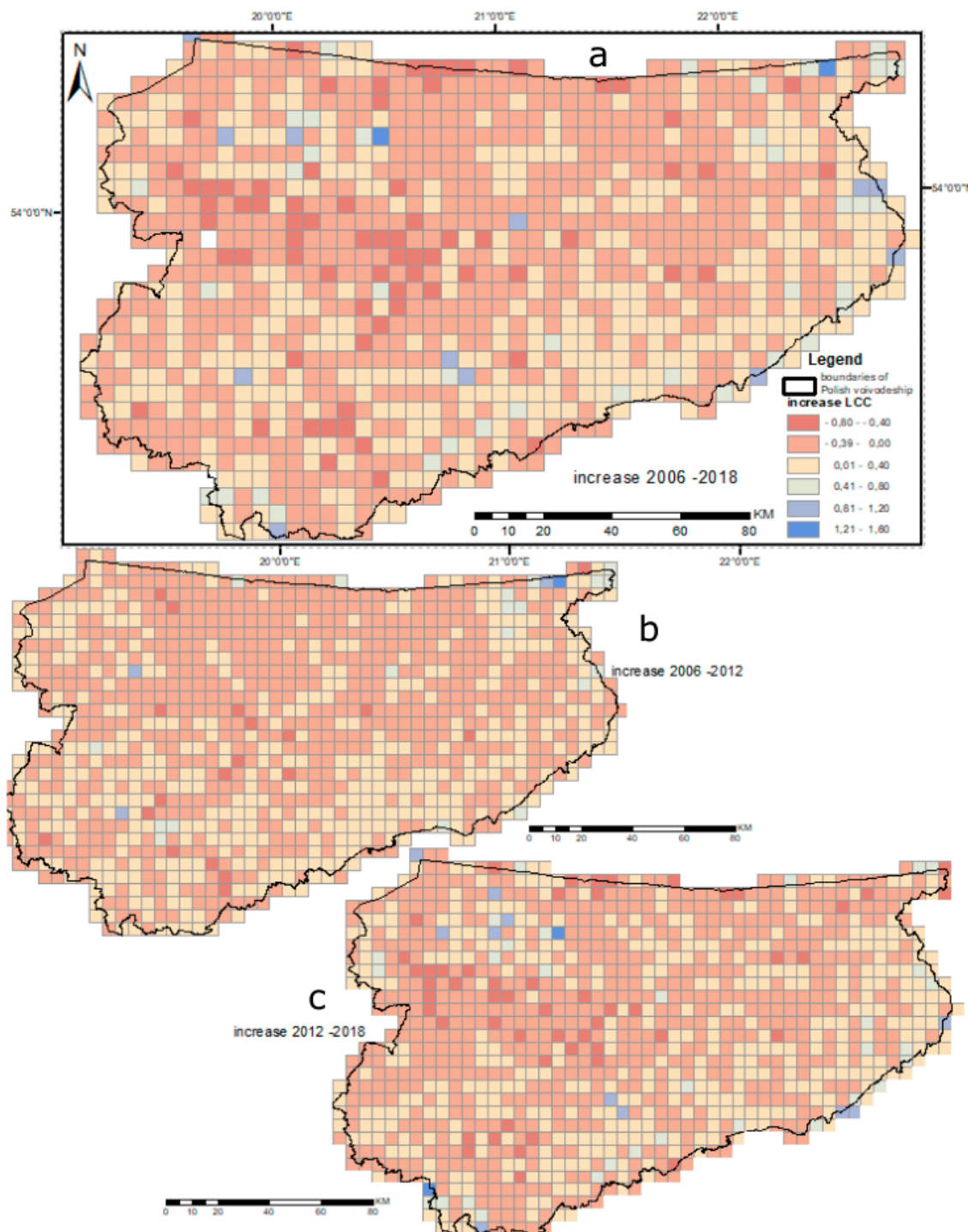


**Figure 5.** Classification of the increase in the values of the LCC indicator based on data for 2006–2018 (a), 2006–2012 (b), and 2018 (c).

#### 4. Discussion

The results of the analysis revealed that land cover continuity decreased in the entire Region of Warmia and Mazury between 2006 and 2018. The largest classes (4 and 5) accounted for more than 70% of all EUM, which points to considerable variations in land cover within an area of 25 km<sup>2</sup>. The number of EUM in each class is presented in Figure 6.

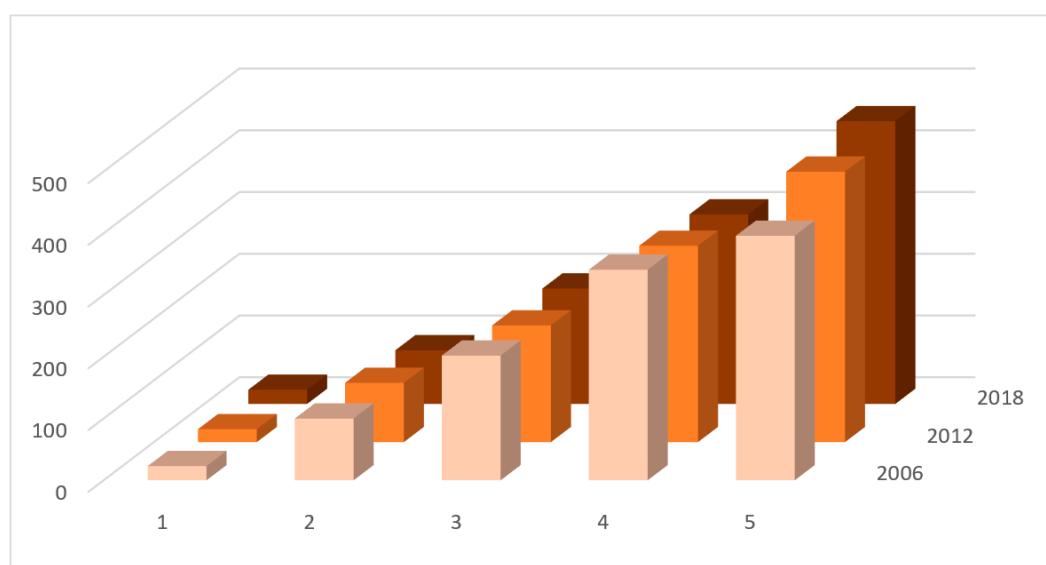


**Figure 6.** Number of EUM in classes.

The greatest increase in the number of EUM was observed in class 5 in 2012. The size of class 5 increased by 10% between 2006 and 2012. A minor decrease was noted in the minimum and mean values of the LCC indicator. The mean values and the number of EUM point to considerable fragmentation of land cover in the analyzed region. This observation can be attributed to the region's development and urbanization, and it is particularly undesirable in EUM localized in areas of high natural value. The data in Figure 4 point to considerable fragmentation of land cover in the studied area. Other high classes (with low values of the LCC indicator) are often localized in the vicinity of large settlements and major transport routes, in particular transit routes that were built or modernized in recent years. The areas with different LC types and the number of EUM in each class in the evaluated years are presented in Table 5. These findings point to an increase in the size of anthropogenically changed areas (CLC class 1—artificial surfaces). Despite the rapid increase in the size of areas with predominantly artificial surfaces, their average area continued to decrease. A decrease was also noted in the average area of other LC types. Average area increased only for farmland (164.09 ha in 2006, 172.05 ha in 2012, 176.62 ha in 2018), but the total area of agricultural land decreased considerably (by nearly 10% between 2006 and 2012, and by another 10% between 2012 and 2018). The observed decrease in the total and average area of ecologically valuable sites (wetlands—CLC class 4, and water bodies—CLC class 5) gives cause for concern. Some of these areas were probably converted to forests (CLC class 3). However, forest area did not increase significantly, and average forest area decreased.

Fragmented urbanization is a highly negative phenomenon. Between 2006 and 2012, the number of anthropogenically changed areas increased from 710 to 1738, whereas their average size decreased from 50.22 ha to 37.38 ha, which points to considerable relaxation of spatial planning policies. Minor land conversion schemes, which generally drive urbanization, were introduced in the analyzed voivodeship. Such programs represent the most undesirable type of land fragmentation. The above observation was confirmed by the values of the LCC indicator which often exceeded 1.00 (CLC classes 4 and 5) in the analyzed period. A smaller, but continued increase in the number of anthropogenically changed areas was noted between 2012 and 2018 when the number of EUM in CLC class 1 increased from 1738 to 1960, and their average size increased to 40.41 ha. This indicates that land development projects proceeded at a slower rate. Unfortunately, the area of development sites created in 2006–2012 continued to increase.

**Table 5.** Size of LCC classes.

2006						2012						2018					
CLC	Area_ha	EUM	CLC Class 1	Total EUM	Average Area	Area_ha	EUM	CLC Class 1	Total EUM	Average Area	Area_ha	EUM	CLC Class 1	Total EUM	Average Area		
111	230.85	3	35,655.17	710	50.22	163.64	2	64,962.05	1738	37.38	169.16	2	79,203.72	1960	40.41		
112	27,891.54	493				53,351.11	1435				63,517.01	1577					
121	2787.39	72				3330.68	81				3817.10	92					
122	286.13	8				523.98	16				1707.64	39					
124	547.64	8				639.27	9				780.11	9					
131	1120.98	32				2089.14	60				2686.85	67					
132	85.29	5				57.44	3				40.98	1					
133	61.54	3				1053.32	23				2483.27	49					
141	182.15	12				213.37	11				272.28	14					
142	2461.68	74	3540.11	98	3729.32	110											
211	1,229,517.42	2549	1,612,813.43	9829	164.09	1,188,293.55	2568	1,531,248.57	8900	172.05	1,165,117.25	2605	1,498,280.42	8483	176.62		
222	240.65	5				313.75	4				306.83	5					
231	185,788.47	2617				194,495.17	2648				195,171.08	2572					
242	69,956.83	2260				37,495.02	1335				34,350.84	1203					
243	127,310.06	2398				110,651.09	2345				103,334.40	2098					
311	120,976.57	1874	819,195.33	6746	121.43	123,218.35	1866	868,103.19	7388	117.50	125,055.82	1876	887,992.39	7453	119.15		
312	420,735.08	1989				429,525.05	1983				431,037.94	1997					
313	244,959.52	2358				257,000.81	2398				276,712.17	2453					
321	2435.58	11				2363.79	9				2508.26	9					
324	29,816.28	508				55,722.89	1126				52,467.51	1114					
331	63.14	2				63.14	2				69.21	2					
333	209.16	4				209.16	4				141.48	2					
411	13,202.14	266	13,831.76	276	50.12	16,077.80	345	16,745.83	356	47.04	17,494.35	377	18,195.61	388	46.90		
412	629.62	10				668.03	11				701.26	11					
511	987.67	23	134,696.12	1100	122.45	902.28	19	137,295.95	1140	120.44	870.40	18	137,640.60	1140	120.74		
512	133,289.12	1075				109,235.42	1098				109,436.72	1099					
521	0.00	0				25,068.69	20				25,243.91	20					
523	419.33	2				2089.57	3				2089.57	3					
Total	2,616,191.81	18,661				2,618,355.59	19,522				2,621,312.73	19,424					

The above observation was confirmed by changes in the value of the LCC indicator for the three analyzed years. The changes in the number of EUM in each class are presented in Figure 7. The greatest difference was noted in class 5 where the values of the LCC indicator changed in 72% of EUM. The above implies that the value of the LCC indicator decreased by around 39% in these units. Considerable changes were also observed in class 4, which aggregated nearly 27% of all EUM between 2006 and 2018. In class 4, the maximum increase in LCC was estimated at 40%. An analysis of the changes in land cover types (Table 5) indicates that some of these EUM contributed to the LCC of artificial surfaces.

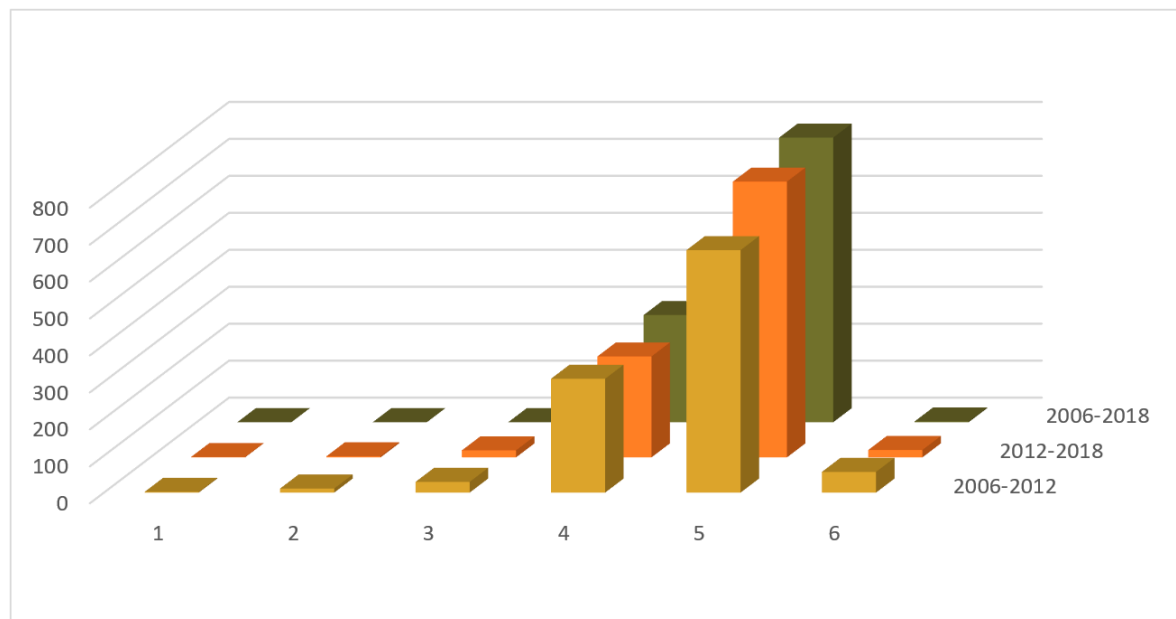


**Figure 7.** LCC classes. 3(a)—classification for 2018 based on CLC classes.

A steep decrease in the values of the LCC indicator was observed between 2006 and 2012. The area of artificial surfaces and the fragmentation of areas with homogeneous land cover continued to increase in the above period. A further decrease in the values of the LCC indicator was noted between 2012 and 2018, and it was accompanied by an increase in the area of artificial surfaces, which, however, was less pronounced than in the previous period. The observed trends were stabilized or even stagnant.

## 5. Conclusions

The continuity of land cover types was analyzed based on CORINE Land Cover data for 2006, 2012, and 2018. The land cover continuity (LCC) indicator was calculated for 1062 equivalent units of measurement (EUM). The rate of changes in the LCC indicator between the analyzed years was determined. Changes in the values of LCC indicators, changes in the area of different land cover types, and changes in the number of EUM with identical land cover types (based on CLC data) were calculated.

The analysis revealed a considerable decrease in the values of the LCC indicator, which, combined with the observed changes in the number and area of EUM, testifies to considerable fragmentation of land cover and high anthropogenic pressure in the studied region.

The results give reason for concern in areas of high natural value, which are found in abundance in the Region of Warmia and Mazury. It should be noted that landscape fragmentation in the southeastern part of the studied region was less pronounced when analyzed with the use of the proposed method than the EEA web map. However, the results of this study indicate that local landscapes are becoming increasingly fragmented, which could be attributed to the large number of CLC land cover types (total of 44). The fragmentation of ecologically valuable sites decreases resistance to anthropogenic pressure,

and some of these areas are at risk of being converted to artificial surfaces. The study also demonstrated that large habitats, in particular forests, are less susceptible to fragmentation, which could imply that the size of different land cover types is directly correlated with their sensitivity to fragmentation. Landscape fragmentation was higher in areas adjacent to cities where transport networks are being developed. The presented findings are consistent with the results of other studies on landscape fragmentation, which indicates that the proposed methodology is correct.

The loss of farming areas is quite alarming because agriculture is still the main source of income in the region. Agricultural land is susceptible to anthropogenic pressure, and farmland area could be expected to decrease in the long-term perspective. The division of agricultural habitats into smaller fragments could also decrease agricultural productivity. These observations clearly indicate that policy makers responsible for spatial planning should implement additional measures to effectively protect farmland in the region.

Land fragmentation analyses based on CLC data supported the identification of development trends in the examined region. The number of anthropogenically changed areas increased between 2006 and 2012. The number of CLC class 1 fields increased by 244%, and their average area decreased by 74%, which points to a highly significant and uncontrolled increase in the number of anthropogenically changed areas that detract from urban consolidation. These processes were clearly slowed down between 2012 and 2018. In that period, the number of newly created development sites increased by only 1%, but their size increased from 37.38 ha to 40.41 ha, which implies that the previously created development sites continued to expand.

These observations testify to the significance of sustainable development policies and measures that prevent land fragmentation. Landscape monitoring supports the identification of land re-parceling trends, which, as demonstrated by this study, tend to spread, exert a negative influence on other land cover types, and contribute to land fragmentation. These findings further underscore the significance of the undertaken research.

The study demonstrated that CORINE Land Cover data are useful for analyses of changes in land cover. Such analyses can be carried out to determine the trends and the extent of changes in geographic space. CORINE Land Cover data have a large territorial scope, and they are gathered, processed, and released in a uniform manner. These data are also periodically updated, which increases their reliability. Despite the fact that the temporal scope of land cover data is the main limitation of the CLC inventory, landscape fragmentation does not proceed rapidly enough to be considerably affected by the lack of more frequent data updates. The CLC inventory supports observations of changes in land cover across seemingly similar categories, such as the transformation of meadows and pastures into urban green spaces. These processes could lead to far-reaching changes not only in landscape, but also in the economic and social use of land.

Most studies on land fragmentation focus on analyses of habitat patches and wildlife corridors, whereas other areas are regarded merely as a backdrop. The main novelty of the presented research is that all land cover types are taken into consideration in the analysis of landscape fragmentation. This study demonstrated that fragmentation affects all types of land cover. This process could be desirable in some cases, but it can also pose a considerable risk in certain areas. The CLC inventory is a widely available source of valuable data that is easy to transform and can be deployed to study various areas. Planning experts and local governments can rely on the CLC database to monitor changes in space. Landscape fragmentation should be regularly monitored to prevent uncontrolled spatial transformations, preserve habitat continuity, and ensure the continuity of desirable spatial processes.

**Author Contributions:** Conceptualization, I.C.; Methodology, I.C.; Data curation, A.B.; Investigation, A.B.; Formal analysis, A.Ž.-S.; Writing—original draft, A.Ž.-S.; Supervision, M.Z.; Writing—editing and review, M.Z. All authors have read and agreed to the published version of the manuscript.

**Funding:** This research received no external funding.

**Conflicts of Interest:** The authors declare no conflict of interest.

## References

- Wei, T.; Shangguan, D.; Shen, X.; Ding, Y.; Yi, S. Dynamics of Land Use and Land Cover Changes in An Arid Piedmont Plain in the Middle Reaches of the Kaxgar River Basin, Xinjiang, China. *ISPRS Int. J. Geo-Inf.* **2020**, *9*, 87. [\[CrossRef\]](#)
- Pelorosso, R.; Leone, A.; Boccia, L. Land cover and land use change in the Italian central Apennines: A comparison of assessment methods. *Appl. Geogr.* **2009**, *29*, 35–48. [\[CrossRef\]](#)
- Cieślak, I. *Multifaceted Analysis of Land Use Conflict*; Wydawnictwo UWM: Olsztyn, Poland, 2018. (In Polish)
- Cieślak, I.; Szuniewicz, K. The quality of pedestrian space in the city: A case study of Olsztyn. *Bull. Geogr. Socio-Econ. Ser.* **2015**, *30*, 31–42. [\[CrossRef\]](#)
- Wubie, M.A.; Assen, M.; Nicolau, M.D. Patterns, causes and consequences of land use/cover dynamics in the Gumara watershed of lake Tana basin, Northwestern Ethiopia. *Environ. Syst. Res.* **2016**, *5*. [\[CrossRef\]](#)
- Petrisor, A.-I.; Sirodoev, I.; Ianos, I. Trends in the National and Regional Transitional Dynamics of Land Cover and Use Changes in Romania. *Remote Sens.* **2020**, *12*, 230. [\[CrossRef\]](#)
- Büttner, H. The Stakeholder Dialogue in the Third Project Phase of GLOWA-Danube. In *Regional Assessment of Global Change Impacts*; Springer Science and Business Media LLC: Berlin/Heidelberg, Germany, 2016; pp. 49–53.
- Soto-Berelov, M.; Madsen, K. Continuity and Distinction in Land Cover Across a Rural Stretch of the U.S.-Mexico Border. *Hum. Ecol.* **2011**, *39*, 509–526. [\[CrossRef\]](#)
- Fahrig, L. Effects of Habitat Fragmentation on Biodiversity. *Annu. Rev. Ecol. Evol. Syst.* **2003**, *34*, 487–515. [\[CrossRef\]](#)
- Cieślak, I. *Contemporary Valorisation of Urban Space*; Wydawnictwo UWM: Olsztyn, Poland, 2012. (In Polish)
- Bennett, A.F.; Saunders, D.A. Habitat fragmentation and landscape change. In *Conservation Biology for All*; Oxford University Press (OUP): Oxford, UK, 2010; pp. 88–106.
- Lambin, E.F.; Turner, B.; Geist, H.J.; Agbola, S.B.; Angelsen, A.; Bruce, J.W.; Coomes, O.T.; Dirzo, R.; Fischer, G.; Folke, C.; et al. The causes of land-use and land-cover change: Moving beyond the myths. *Glob. Environ. Chang.* **2001**, *11*, 261–269. [\[CrossRef\]](#)
- Aye, K.S.; Htay, K.K. The Impact of Land Cover Changes on Socio-economic Conditions in Bawlakhe District, Kayah State. In *Environmental Law and Policies in Turkey*; Springer Science and Business Media LLC: Berlin/Heidelberg, Germany, 2019; pp. 239–258.
- Nath, B.; Niu, Z.; Singh, R.P. Land Use and Land Cover Changes, and Environment and Risk Evaluation of Dujiangyan City (SW China) Using Remote Sensing and GIS Techniques. *Sustainability* **2018**, *10*, 4631. [\[CrossRef\]](#)
- Villoria, N.B. Technology Spillovers and Land Use Change: Empirical Evidence from Global Agriculture. *Am. J. Agric. Econ.* **2019**, *101*, 870–893. [\[CrossRef\]](#)
- Lambin, E.F.; Meyfroidt, P. Global land use change, economic globalization, and the looming land scarcity. *Proc. Natl. Acad. Sci. USA* **2011**, *108*, 3465–3472. [\[CrossRef\]](#) [\[PubMed\]](#)
- Lone, S.A.; Mayer, I.A. Geo-spatial analysis of land use/land cover change and its impact on the food security in District Anantnag of Kashmir Valley. *Int. J. Geomat. Geosci.* **2018**, *84*, 785–794. [\[CrossRef\]](#)
- Ahmad, N.; Sinha, D.K.; Singh, K.M. Changes in land use pattern and factors responsible for variations in current fallow land in Bihar, India. *Indian J. Agric. Res.* **2018**, *52*, 236–242. [\[CrossRef\]](#)
- Wan, L.; Zhang, Y.; Zhang, X.; Qi, S.; Na, X. Comparison of land use/land cover change and landscape patterns in Honghe National Nature Reserve and the surrounding Jiansanjiang Region, China. *Ecol. Indic.* **2015**, *51*, 205–214. [\[CrossRef\]](#)
- Nagendra, H.; Munroe, D.; Southworth, J. From pattern to process: Landscape fragmentation and the analysis of land use/land cover change. *Agric. Ecosyst. Environ.* **2004**, *101*, 111–115. [\[CrossRef\]](#)
- Gardi, C. (Ed.) *Urban Expansion, Land Cover and Soil Ecosystem Services*; Routledge: London, UK, 2017; p. 332.
- Biological consequences of ecosystem fragmentation: A review. *Biol. Conserv.* **1992**, *59*, 77. [\[CrossRef\]](#)
- Dytham, C.; Forman, R.T.T. Land Mosaics: The Ecology of Landscapes and Regions. *J. Ecol.* **1996**, *84*, 787. [\[CrossRef\]](#)
- Jaeger, J.A. Landscape division, splitting index, and effective mesh size: New measures of landscape fragmentation. *Landsc. Ecol.* **2000**, *15*, 115–130. [\[CrossRef\]](#)

25. EEA/FOEN. *Landscape Fragmentation in Europe. Joint EEA-FOEN Report. European Environment Agency and Federal Office for the Environment; Office for Official Publications of the European Union: Luxembourg*, 2011; p. 87.
26. Jaeger, J.A.G.; Bertiller, R.; Schwick, C.; Müller, K.; Steinmeier, C.; Ewald, K.C.; Ghazoul, J. Implementing Landscape Fragmentation as an Indicator in the Swiss Monitoring System of Sustainable Development (Monet). *J. Environ. Manag.* **2008**, *88*, 737–751. [\[CrossRef\]](#)
27. McGarigal, K.; Marks, B.J. *FRAGSTATS: Spatial Pattern Analysis Program for Quantifying Landscape Structure*; USDA Forest Service: Dolores, CO, USA, 1995; Volume 351, pp. 9–12.
28. Low, S.M. Towards a theory of urban fragmentation: A cross-cultural analysis of fear, privatization, and the state. *Cybergeogeo* **2006**, 2006. [\[CrossRef\]](#)
29. Carmona, M. Re-theorising contemporary public space: A new narrative and a new normative. *J. Urban. Int. Res. Placemaking Urban Sustain.* **2014**, *8*, 373–405. [\[CrossRef\]](#)
30. Tomaselli, V.; Tenerelli, P.; Sciandrello, S. Mapping and quantifying habitat fragmentation in small coastal areas: A case study of three protected wetlands in Apulia (Italy). *Environ. Monit. Assess.* **2011**, *184*, 693–713. [\[CrossRef\]](#) [\[PubMed\]](#)
31. Landscape Fragmentation Pressure and Trends in Europe. Available online: [www.eea.europa.eu/data-and-maps/indicators/mobility-and-urbanisation-pressure-on-ecosystems-2/assessment](http://www.eea.europa.eu/data-and-maps/indicators/mobility-and-urbanisation-pressure-on-ecosystems-2/assessment) (accessed on 14 April 2020).
32. Llausàs, A.; Nogué, J. Indicators of landscape fragmentation: The case for combining ecological indices and the perceptive approach. *Ecol. Indic.* **2012**, *15*, 85–91. [\[CrossRef\]](#)
33. Walz, U. Indicators to monitor the structural diversity of landscapes. *Ecol. Model.* **2015**, *295*, 88–106. [\[CrossRef\]](#)
34. Arnot, C.; Fisher, P.; Wadsworth, R.; Wellens, J. Landscape metrics with ecotones: Pattern under uncertainty. *Landsc. Ecol.* **2004**, *19*, 181–195. [\[CrossRef\]](#)
35. Levin, N.; Lahav, H.; Ramon, U.; Heller, A.; Nizry, G.; Tsoar, A.; Sagi, Y. Landscape continuity analysis: A new approach to conservation planning in Israel. *Landsc. Urban Plan.* **2007**, *79*, 53–64. [\[CrossRef\]](#)
36. Jürgenson, E. Land reform, land fragmentation and perspectives for future land consolidation in Estonia. *Land Use Policy* **2016**, *57*, 34–43. [\[CrossRef\]](#)
37. Szuniewicz, K.S. THE USE OF WEBGIS SERVICES IN PUBLIC ADMINISTRATION IN POLAND. In *Proceedings of the 15th International Multidisciplinary Scientific GeoConference SGEM2015, Informatics, Geoinformatics and Remote Sensing*; STEF92 Technology: Albena, Bulgaria, 2011.
38. Bilozor, A.; Czyża, S.; Bajerowski, T. Identification and Location of a Transitional Zone between an Urban and a Rural Area Using Fuzzy Set Theory, CLC, and HRL Data. *Sustainability* **2019**, *11*, 7014. [\[CrossRef\]](#)
39. Cieślak, I.; Bilozor, A.; Szuniewicz, K. The Use of the CORINE Land Cover (CLC) Database for Analyzing Urban Sprawl. *Remote Sens.* **2020**, *12*, 282. [\[CrossRef\]](#)
40. Balázs, P.; Konkoly-Gyuró, É.; Wrba, T. Land cover continuity as a tool for nature conservation. *Verh. Der Zool Ges. Österreich* **2016**, *153*, 47–65.
41. Brown, G.; Raymond, C.M. Methods for identifying land use conflict potential using participatory mapping. *Landsc. Urban Plan.* **2014**, *122*, 196–208. [\[CrossRef\]](#)
42. Melchiorri, M.; Florczyk, A.J.; Freire, S.; Schiavina, M.; Pesaresi, M.; Kemper, T. Unveiling 25 Years of Planetary Urbanization with Remote Sensing: Perspectives from the Global Human Settlement Layer. *Remote Sens.* **2018**, *10*, 768. [\[CrossRef\]](#)
43. Puniach, E.; Bieda, A.; Ćwiakala, P.; Kwartnik-Pruc, A.; Parzych, P. Use of Unmanned Aerial Vehicles (UAVs) for Updating Farmland Cadastral Data in Areas Subject to Landslides. *ISPRS Int. J. Geo-Inf.* **2018**, *7*, 331. [\[CrossRef\]](#)
44. Schug, F.; Okujeni, A.; Hauer, J.; Hostert, P.; Nielsen, J.Ø.; Van Der Linden, S. Mapping patterns of urban development in Ouagadougou, Burkina Faso, using machine learning regression modeling with bi-seasonal Landsat time series. *Remote Sens. Environ.* **2018**, *210*, 217–228. [\[CrossRef\]](#)
45. Benedetti, A.; Picchiani, M.; Del Frate, F. Sentinel-1 and Sentinel-2 Data Fusion for Urban Change Detection. In *Proceedings of the IGARSS 2018–2018 IEEE International Geoscience and Remote Sensing Symposium, Valencia, Spain, 23–27 July 2018*; pp. 1962–1965. [\[CrossRef\]](#)

46. Lefebvre, A.; Sannier, C.; Corpetti, T. Monitoring Urban Areas with Sentinel-2A Data: Application to the Update of the Copernicus High Resolution Layer Imperviousness Degree. *Remote Sens.* **2016**, *8*, 606. [\[CrossRef\]](#)
47. Liu, X.; Hu, G.; Chen, Y.; Li, X.; Xu, X.; Li, S.; Pei, F.; Wang, S. High-resolution multi-temporal mapping of global urban land using Landsat images based on the Google Earth Engine Platform. *Remote Sens. Environ.* **2018**, *209*, 227–239. [\[CrossRef\]](#)
48. Che, M.; Gamba, P. Intra-Urban Change Analysis Using Sentinel-1 and Nighttime Light Data. *IEEE J. Sel. Top. Appl. Earth Obs. Remote Sens.* **2019**, *12*, 1134–1142. [\[CrossRef\]](#)
49. Akay, S.S.; Sertel, E. URBAN LAND COVER/USE CHANGE DETECTION USING HIGH RESOLUTION SPOT 5 AND SPOT 6 IMAGES AND URBAN ATLAS NOMENCLATURE. *ISPRS-Int. Arch. Photogramm. Remote Sens. Spat. Inf. Sci.* **2016**, 789–796. [\[CrossRef\]](#)
50. Luo, X.; Tong, X.; Qian, Z.; Pan, H.; Liu, S. Detecting urban ecological land-cover structure using remotely sensed imagery: A multi-area study focusing on metropolitan inner cities. *Int. J. Appl. Earth Obs. Geoinf.* **2019**, *75*, 106–117. [\[CrossRef\]](#)
51. Benz, U.C.; Hofmann, P.; Willhauck, G.; Lingenfelder, I.; Heynen, M. Multi-resolution, object-oriented fuzzy analysis of remote sensing data for GIS-ready information. *ISPRS J. Photogramm. Remote Sens.* **2004**, *58*, 239–258. [\[CrossRef\]](#)
52. Washaya, P.; Balz, T. SAR COHERENCE CHANGE DETECTION OF URBAN AREAS AFFECTED BY DISASTERS USING SENTINEL-1 IMAGERY. *ISPRS-Int. Arch. Photogramm. Remote Sens. Spat. Inf. Sci.* **2018**, 1857–1861. [\[CrossRef\]](#)
53. Kuc, G.; Chormański, J. Sentinel-2 imagery for mapping and monitoring imperviousness in urban areas. In Proceedings of the International Archives of the Photogrammetry, Remote Sensing and Spatial Information Sciences, Volume XLII-1/W2, 2019 Evaluation and Benchmarking Sensors, Systems and Geospatial Data in Photogrammetry and Remote Sensing, Warsaw, Poland, 16–17 September 2019.
54. Liu, Z.; He, C.; Zhang, Q.; Huang, Q.; Yang, Y. Extracting the dynamics of urban expansion in China using DMSP-OLS nighttime light data from 1992 to 2008. *Landsc. Urban Plan.* **2012**, *106*, 62–72. [\[CrossRef\]](#)
55. Ma, T.; Zhou, C.; Pei, T.; Haynie, S.; Fan, J. Quantitative estimation of urbanization dynamics using time series of DMSP/OLS nighttime light data: A comparative case study from China's cities. *Remote Sens. Environ.* **2012**, *124*, 99–107. [\[CrossRef\]](#)
56. Gao, B.; Huang, Q.; He, C.; Dou, Y. Similarities and differences of city-size distributions in three main urban agglomerations of China from 1992 to 2015: A comparative study based on nighttime light data. *J. Geogr. Sci.* **2017**, *27*, 533–545. [\[CrossRef\]](#)
57. Deng, J.; Huang, Y.; Chen, B.; Tong, C.; Liu, P.; Wang, H.; Hong, Y. A Methodology to Monitor Urban Expansion and Green Space Change Using a Time Series of Multi-Sensor SPOT and Sentinel-2A Images. *Remote Sens.* **2019**, *11*, 1230. [\[CrossRef\]](#)
58. Li, X.; Zhou, Y. Urban mapping using DMSP/OLS stable night-time light: A review. *Int. J. Remote Sens.* **2017**, *38*, 6030–6046. [\[CrossRef\]](#)
59. Zhao, J.; Ji, G.; Yue, Y.; Lai, Z.; Chen, Y.; Yang, D.; Yang, X.; Wang, Z. Spatio-temporal dynamics of urban residential CO<sub>2</sub> emissions and their driving forces in China using the integrated two nighttime light datasets. *Appl. Energy* **2019**, *235*, 612–624. [\[CrossRef\]](#)
60. Jones, C.; Kammen, D.M. Spatial Distribution of U.S. Household Carbon Footprints Reveals Suburbanization Undermines Greenhouse Gas Benefits of Urban Population Density. *Environ. Sci. Technol.* **2014**, *48*, 895–902. [\[CrossRef\]](#)
61. Cao, Y.; Wang, Y.; Li, G.; Fang, X. Vegetation Response to Urban Landscape Spatial Pattern Change in the Yangtze River Delta, China. *Sustainability* **2019**, *12*, 68. [\[CrossRef\]](#)
62. Stathopoulou, M.; Cartalis, C.; Petrakis, M. Integrating Corine Land Cover data and Landsat TM for surface emissivity definition: Application to the urban area of Athens, Greece. *Int. J. Remote Sens.* **2007**, *28*, 3291–3304. [\[CrossRef\]](#)
63. Cieślak, I.; Szuniewicz, K.; Pawlewicz, K.; Czyża, S. Land Use Changes Monitoring with CORINE Land Cover Data. *IOP Conf. Ser. Mater. Sci. Eng.* **2017**, *245*, 52049. [\[CrossRef\]](#)
64. Amato, F.; Tonini, M.; Murgante, B.; Kanevski, M. Fuzzy definition of Rural Urban Interface: An application based on land use change scenarios in Portugal. *Environ. Model. Softw.* **2018**, *104*, 171–187. [\[CrossRef\]](#)

65. Danielaini, T.T.; Maheshwari, B.; Hagare, D. Defining rural–urban interfaces for understanding ecohydrological processes in West Java, Indonesia: Part II. Its application to quantify rural–urban interface ecohydrology. *Ecohydrol. Hydrobiol.* **2018**, *18*, 37–51. [\[CrossRef\]](#)
66. Hu, T.; Yang, J.; Li, X.; Gong, P. Mapping urban land use by using landsat images and open social data. *Remote Sens.* **2016**, *8*, 151. [\[CrossRef\]](#)
67. AlQurashi, A.F.; Kumar, L. Investigating the Use of Remote Sensing and GIS Techniques to Detect Land Use and Land Cover Change: A Review. *Adv. Remote Sens.* **2013**, *2*, 193–204. [\[CrossRef\]](#)
68. Rogan, J.; Chen, D. Remote sensing technology for mapping and monitoring land-cover and land-use change. *Prog. Plan.* **2004**, *61*, 301–325. [\[CrossRef\]](#)
69. Gauthier, D.A.; Wiken, E.B. Monitoring the conservation of grassland habitats, Prairie Ecozone, Canada. *Environ. Monit. Assess.* **2003**, *88*, 343–364. [\[CrossRef\]](#) [\[PubMed\]](#)
70. Kupfer, J.A. National assessments of forest fragmentation in the US. *Glob. Environ. Chang.* **2006**, *16*, 73–82. [\[CrossRef\]](#)
71. Fischer, J.; Lindenmayer, D. Landscape modification and habitat fragmentation: A synthesis. *Glob. Ecol. Biogeogr.* **2007**, *16*, 265–280. [\[CrossRef\]](#)
72. Saura, S.; Estreguil, C.; Mouton, C.; Rodríguez-Freire, M. Network analysis to assess landscape connectivity trends: Application to European forests (1990–2000). *Ecol. Indic.* **2011**, *11*, 407–416. [\[CrossRef\]](#)
73. De Montis, A.; Martín, B.; Ortega, E.; Ledda, A.; Serra, V.; Perez, E.O. Landscape fragmentation in Mediterranean Europe: A comparative approach. *Land Use Policy* **2017**, *64*, 83–94. [\[CrossRef\]](#)
74. Moser, B.; Jaeger, J.A.G.; Tappeiner, U.; Tasser, E.; Eiselt, B. Modification of the effective mesh size for measuring landscape fragmentation to solve the boundary problem. *Landsc. Ecol.* **2006**, *22*, 447–459. [\[CrossRef\]](#)
75. Senetra, A.; Szczepańska, A.; Wasilewicz-Pszczółkowska, M. Analysis of changes in the land use structure of developed and urban areas in Eastern Poland. *Bull. Geogr. Socio-Econ. Ser.* **2014**, *24*, 219–230. [\[CrossRef\]](#)
76. Bechtel, B.; Pesaresi, M.; See, L.; Mills, G.; Ching, J.; Alexander, P.J.; Feddema, J.; Florczyk, A.J.; Stewart, I. TOWARDS CONSISTENT MAPPING OF URBAN STRUCTURES–GLOBAL HUMAN SETTLEMENT LAYER AND LOCAL CLIMATE ZONES. *ISPRS-Int. Arch. Photogramm. Remote Sens. Spat. Inf. Sci.* **2016**, 1371–1378. [\[CrossRef\]](#)
77. Yilmaz, R. Monitoring land use/land cover changes using CORINE land cover data: A case study of Silivri coastal zone in Metropolitan Istanbul. *Environ. Monit. Assess.* **2009**, *165*, 603–615. [\[CrossRef\]](#) [\[PubMed\]](#)
78. Feranec, J.; Hazeu, G.; Christensen, S.; Jaffrain, G. Corine land cover change detection in Europe (case studies of the Netherlands and Slovakia). *Land Use Policy* **2007**, *24*, 234–247. [\[CrossRef\]](#)
79. Pirowski, T.; Timek, M. Analysis of land use and land cover maps suitability for modeling population density of urban areas—redistribution to new spatial units based on CLC and UA databases. *Geoinform. Pol.* **2018**, *17*, 53–64. [\[CrossRef\]](#)
80. Chery, P.; Lee, A.; Commagnac, L.; Thomas-Chery, A.-L.; Jalabert, S.; Slak, M.-F. Impact de l’artificialisation sur les ressources en sol et les milieux en France métropolitaine. *Cybergeo* **2014**, *668*, 1–27. [\[CrossRef\]](#)
81. Jucha, W.; Krocak, R. Comparison Land Use Database between CORINE Land Cover Programme and Data from Orthophotomaps Vectorization. In *Spoleczno-ekonomiczne i Przestrzenne Przemiany Struktur Regionalnych Vol. 2*; Kaczmarek, E., Raźniak, P., Eds.; Oficyna Wydawnicza AFM: Kraków, Poland, 2014; pp. 123–136. (In Polish)
82. Pașca, A.; Năsu, D. The use of Corine Land Cover 2012 and Urban Atlas 2012 databases in agricultural spatial analysis. Case study: Cluj County, Romania. *Res. J. Agric. Sci.* **2016**, *48*, 314–322.
83. Weng, Q. *Remote Sensing for Sustainability*; Routledge: London, UK, 2016; p. 357.
84. Cieślak, I.; Szuniewicz, K. Analysis of the investment potential of location using the AHP method. *Géod. Vestník* **2018**, *62*, 279–292. [\[CrossRef\]](#)
85. Meneses, B.; Reis, E.; Reis, R.; Vale, M.J. The Effects of Land Use and Land Cover Geoinformation Raster Generalization in the Analysis of LUCC in Portugal. *ISPRS Int. J. Geo-Inf.* **2018**, *7*, 390. [\[CrossRef\]](#)
86. Hartvigsen, M. Land reform and land fragmentation in Central and Eastern Europe. *Land Use Policy* **2014**, *36*, 330–341. [\[CrossRef\]](#)
87. Cieślak, I.; Pawlewicz, K.; Pawlewicz, A.; Szuniewicz, K. Impact of the natura 2000 network on social-economic development of rural communes in Poland. *Res. Rural Dev.* **2015**, *2*, 169–175.

88. Szamrowski, P.; Pawlewicz, A.; Pawlewicz, K. Environmental and Natural Heritages Investments in Fisheries Local Action Groups (FLAGs) Functioning in the Warmia and Masuria Region. In *Proceedings of the 9th International Conference "Environmental Engineering 2014"*; Vilnius Gediminas Technical University: Vilnius, Lithuania, 2014.
89. Lizińska, W.; Waldziński, D. Development strategy of the Warmian-Masurian Voivodeship in the context of European integration. Working Papers/Uniwersytet Gdański. *Ośrodek Badań Integr. Eur.* **2002**, *2*, 22–30. (In Polish)
90. Zielińska-Szczepkowska, J.; Żróbek-Różańska, A. Activity of local authorities in the face of demographic changes shaping the tourism sector. An example of the Warmian-Masurian Voivodeship. *Zesz. Nauk. Uniw. Szczecińskiego* **2014**, *826*, 315–323. (In Polish)
91. Board of the Warmian-Masurian Voivodeship. *Strategy of Socio-Economic Development of the Warmian-Masurian Voivodeship until 2025*; Board of the Warmian-Masurian Voivodeship: Olsztyn, Poland, 2015. (In Polish)
92. Pesaresi, M.; Corbane, C.; Julea, A.; Florczyk, A.J.; Syrris, V.; Soille, P. Assessment of the Added-Value of Sentinel-2 for Detecting Built-up Areas. *Remote Sens.* **2016**, *8*, 299. [\[CrossRef\]](#)
93. Klotz, M.; Kemper, T.; Geis, C.; Esch, T.; Taubenböck, H. How good is the map? A multi-scale cross-comparison framework for global settlement layers: Evidence from Central Europe. *Remote Sens. Environ.* **2016**, *178*, 191–212. [\[CrossRef\]](#)
94. Esch, T.; Heldens, W.; Hirner, A.; Keil, M.; Marconcini, M.; Roth, A.; Zeidler, J.; Dech, S.; Strano, E. Breaking new ground in mapping human settlements from space—The Global Urban Footprint. *ISPRS J. Photogramm. Remote Sens.* **2017**, *134*, 30–42. [\[CrossRef\]](#)
95. Levin, N.; Singer, M.; Lai, P.-C. Incorporating Topography into Landscape Continuity Analysis—Hong Kong Island as a Case Study. *Land* **2013**, *2*, 550–572. [\[CrossRef\]](#)
96. Marzęcki, W. *Cultural Continuity in Shaping Urban Space: Characteristics and Method of Evaluating the Quality and Variation of This Space*; Wydawnictwo Uczelniane Politechniki Szczecińskiej: Szczecin, Poland, 2002. (In Polish)
97. Shannon, C.E. *The Mathematical Theory of Communication*, by CE Shannon (and Recent Contributions to the Mathematical Theory of Communication); Weaver, W., Ed.; University of Illinois Press: Champaign, IL, USA, 1949.
98. Pontius, G.P., Jr. European Landscape Dynamics: Corine Land Cover Data. *Photogramm. Eng. Remote Sens.* **2017**, *83*, 79. [\[CrossRef\]](#)
99. Cieślak, I. Identification of areas exposed to land use conflict with the use of multiple-criteria decision-making methods. *Land Use Policy* **2019**, *89*, 104225. [\[CrossRef\]](#)
100. Cieślak, I. Spatial conflicts: Analyzing a burden created by differing land use. *Acta Geogr. Slov.* **2019**, *59*. [\[CrossRef\]](#)
101. Yüksel, A.; Akay, A.E.; Gundogan, R. Using ASTER Imagery in Land Use/cover Classification of Eastern Mediterranean Landscapes According to CORINE Land Cover Project. *Sensors* **2008**, *8*, 1237–1251. [\[CrossRef\]](#) [\[PubMed\]](#)
102. CORINE Land Cover. Available online: [clc.gios.gov.pl](http://clc.gios.gov.pl) (accessed on 20 June 2019).
103. Golenia, M.; Zagajewski, B.; Ochtyra, A.; Hoscilo, A. Semiautomatic land cover mapping according to the 2nd level of the CORINE Land Cover legend. *Pol. Cartogr. Rev.* **2015**, *47*, 203–212. [\[CrossRef\]](#)
104. Balzter, H.; Cole, B.; Thiel, C.; Schmullius, C. Mapping CORINE Land Cover from Sentinel-1A SAR and SRTM Digital Elevation Model Data using Random Forests. *Remote Sens.* **2015**, *7*, 14876–14898. [\[CrossRef\]](#)
105. Jenks, G.F.; Caspall, F.C. ERROR ON CHOROPLETHIC MAPS: DEFINITION, MEASUREMENT, REDUCTION. *Ann. Assoc. Am. Geogr.* **1971**, *61*, 217–244. [\[CrossRef\]](#)
106. Carrão, H.; Singleton, A.; Naumann, G.; Barbosa, P.; Vogt, J.V. An Optimized System for the Classification of Meteorological Drought Intensity with Applications in Drought Frequency Analysis. *J. Appl. Meteorol. Clim.* **2014**, *53*, 1943–1960. [\[CrossRef\]](#)

